

A deep learning approach to increase the value of satellite data for PM_{2.5} monitoring in China

Bo Li, Cheng Liu, Qihou Hu, Mingzhai Sun, Chengxin Zhang, Shulin Zhang, Yizhi Zhu, Ting

Liu, Yike Guo, Martin G. Schultz, Gregory R. Carmichael, Meng Gao

This file includes:

- **Figure. S1. Validation of meteorological parameters simulated by WRF with observation data at ISD (Integrated Surface Database) stations.** (a) temperature. (b) pressure. (c) wind speeds.
- **Figure. S2. The architecture of the ST-NN model. Data include AOD, meteorological data and geographic data.** All the input variables have the 4-D dimensions as [N, lat_size, lon_size, channel]. N means the batch size, lat_size and lon_size means the scale of the data at latitude and longitude, channels mean the types or the height/time dimension of the data. And considering the computational efficiency and the generalization ability of the model, we choose N as 4.
- **Figure. S3. Locations and spatial range of major study regions.** Study regions include North China, East China, South China, Sichuan Basin and Shaanxi Province.
- **Figure. S4. The annual average distribution of PM_{2.5} in Beijing.** It can be seen that the main pollution comes from the southwest, significantly influenced by topography and transmission.

- Figure. S5. ST-NN model predicted and ground-level observed (not used in training) time series of PM_{2.5} in Beijing stations.** (a) Dongsì station in Beijing. (b) Tiantan station in Beijing. (c) Guanyuan station in Beijing. (d) Aotizhognxin station in Beijing. (e) Daxing station in Beijing. (f) Changping station in Beijing. (g) Miyun station in Beijing. (h) Dingling station in Beijing.
- Figure. S6. ST-NN model predicted and ground-level observed (not used in training) time series of PM_{2.5} in China, and comparisons of their diurnal features.** Left column: ST-NN model predicted and ground-level observed (not used in training) time series (2017) of PM_{2.5} in China, and comparisons of their diurnal features. Left column: ST-NN model predicted and observed time series of PM_{2.5} in Wuhan (a1), Suzhou (b1), Zhongshan (c1), Jiangmen (d1), Guanyuan in Beijing (e1), Miyun in Beijing (f1); Right column: ST-NN model predicted and observed diurnal variation of PM_{2.5} in Wuhan (a2), Suzhou (b2), Zhongshan (c2), Jiangmen (d2), Guanyuan in Beijing (e2), Miyun in Beijing (f2).
- Figure.S7. The block distribution of the regional mask validation.** Validation was carried out for different spatial mask scales, the black points are the training sites, and the R-square distribution of the validation sites is enclosed by the solid blue line.
- Figure.S8. Time series of the regional mask performed (Figure.S6b, c, d).** It can be seen that the model can capture pollution effectively.
- Figure. S9. Time series of the regional mask performed (Figure.S6a),** they are the 2°x2° mask validation in the North China. The blue line is the CNEMC data, the orange line is the ST-NN result for clear day, the red line is the ST-NN result for

cloudy day.

- **Figure. S10. Density scatterplots of the ST-NN model** (trained with data from 2017 to 2020 and test with 2020) with hourly(a),monthly(b),annual(c) validation. The fitting line is in purple, and the 1:1 standard line is the black dotted line.
- **Figure. S11 Relative error of cross validation under different cloud coverage rates.**
- **Figure. S12. The density distribution diagram of changes in predicted $PM_{2.5}$ concentrations as a function of relative humidity in marked cloudy conditions.** (a) North China. (b) East China. (c) South China. (d) Sichuan Basin.
- **Figure. S13. The distribution of predicted annual mean concentrations of $PM_{2.5}$ and the locations of monitoring sites.**
- **Figure. S14. Relative importance indicators (R_r : Relative range; R_g : Relative gradient; R_v : Relative variance; R_{AAD} : Relative average absolute deviation) of input variables for different regions.** (a-d) North China. (e-h) East China. (i-l) South China. (m-p) Sichuan Basin. (q-t) Shaanxi Province.
- **Figure. S15. Results of sensitivity analysis of key variables.**
- **Figure. S16. Relative error varies with $PM_{2.5}$ concentrations in different regions.** Five lines with different colors represent errors for North China, East China, South China, Sichuan Basin, and Shaanxi Province.
- **Figure. S17. The relationship between the mean absolute error of the model and the relative error of different input data.** Seven lines with different colors represent model inputs: pressure, temperature, zonal wind (U), meridional wind (V), boundary

layer height, relative humidity, and AOD.

- **Figure. S18. The performance of the validation data logcosh loss function for models built for different regions.** Five lines with different colors represent results for North China, East China, South China, Sichuan Basin, and Shaanxi Province.
- **Figure. S19. The spatiotemporal distribution of CNEMC observed PM_{2.5} concentrations.** (a) Year 2017. (b) Year 2018. (c) Year 2019. (d) Year 2020. (e) Monthly variations.
- **Table S1.** Number of CNEMC stations at different population densities (people/km²).
- **Table S2.** The occurrences of marked cloudy conditions.
- **Table S3.** Descriptions of considered variables.
- **Table S4.** MODIS MCD12C1 Land Cover Types.
- **Table S5.** Traffic Network classification.
- **Table S6.** Point of Interest classification.
- **Table S7.** The α of bivariate test between each parameter and PM_{2.5}.
- **Table S8.** The spatial ranges of study regions.
- **Table S9.** Major features of previous related studies.
- **Table S10.** The influences of different data quality treatments on the performance of the model.
- **Table S11.** Data quality control status.
- **Table S12.** Statistics of number of stations used for training and testing
- **Table S13.** Validation results for different scales of spatial region mask. Validation results for 1x1, 2x2, 3x3, 4x4 degree masks over a general area.

- **Table.S14.** Hourly validation of Near Real Time model (trained with data from 2017 to 2020 and test with 2020). With overall validation R-square above 0.55, we find that the model validates worse in scenarios with lower surface PM_{2.5} concentrations, mainly due to the large uncertainty in both the CNEMC site and satellite aerosol products at low PM_{2.5} concentrations.
- **Table.S15.** Assess the ability of the model to capture different levels of contamination through accuracy and precision. Accuracy and precision rates are defined under. The model results and national control site results are divided according to thresholds, with values greater than the threshold defined as positive samples and values less than the threshold defined as negative samples. The model result and the national control site are both positive samples are defined as TP, the model result is a positive sample and the national control site is a negative sample is defined as FP. The model result and the national control site are both negative samples defined as FN, the model result is a negative sample, and the national control site is a positive sample defined as TN.

$$Accuracy = \frac{TP + TN}{TP + TN + FP + FN}$$

$$Precision = \frac{TP}{TP + FP}$$

Table S1. Number of CNEMC stations at different population densities (people/km²) and the area percentage of different population densities (within parentheses).

	<1	1~25	25~100	100~500	500~1000	>1000
North China	0(7)	2(18)	0(25)	12(30)	37(16)	125(4)
East China	0(3)	0(0)	1(6)	39(59)	56(25)	247(7)
South China	0(13)	0(0)	5(7)	37(69)	45(7)	150(4)
Sichuan Basin	0(0)	0(25)	7(17)	33(48)	54(8)	51(2)

Shaanxi Province 0(0) 0(7) 0(30) 41(52) 35(9) 101(2)

Table S2. The occurrences of marked cloudy conditions.

	2017	Spring	Summer	Autumn	Winter	Year
MODIS	North China	0.62	0.66	0.60	0.83	0.67
	Eastern China	0.66	0.76	0.71	0.69	0.71
	South China	0.86	0.88	0.79	0.77	0.83
	Sichuan Basin	0.81	0.80	0.84	0.83	0.82
	Shaanxi Province	0.66	0.66	0.68	0.74	0.68

Table S3. Descriptions of considered variables.

Product	Unit	Variable Definition	Spatial Resolution	Temporal Resolution
AOD		Aerosol optical depth	0.05°×0.05°	1hour
Tempc	°C	Temperature	0.05°×0.05°×12	1hour
RH	%	Relative Humidity	0.05°×0.05°×12	1hour
HPBL	m	Planetary Boundary Layer Height	0.05°×0.05°	1hour
P	Hpa	Pressure	0.05°×0.05°×12	1hour
U	m/s	Wind Speed (U)	0.05°×0.05°×12	1hour
V	m/s	Wind Speed (V)	0.05°×0.05°×12	1hour
DEM	m	Digital Elevation Model	0.01°×0.01°	Annual
POI		Point of Interest	0.01°×0.01°	Annual
Traffic Network		Traffic Network	0.01°×0.01°	Annual
GDP	¥ /km ²	Gross Domestic Product	0.01°×0.01°	Annual
TPOP	people/km ²	population density	0.01°×0.01°	Annual
Land Cover Type		Land Cover Type	0.05°×0.05°	Annual

Table S4. MODIS MCD12C1 Land Cover Type

Class	Description	Class	Description
0	water	9	savannas
1	evergreen needleleaf forest	10	grasslands
2	evergreen broadleaf forest	11	permanent wetlands
3	deciduous needleleaf forest	12	croplands
4	deciduous broadleaf forest	13	urban and built-up
5	mixed forests	14	cropland/natural vegetation mosaic
6	closed shrubland	15	snow and ice
7	open shrublands	16	barren or sparsely vegetated
8	woody savannas		

Table S5. Traffic Network classification.

Class	Description	Class	Description
0	primary	5	track
0	primary_link	5	track_grade
1	secondary	6	trunk
1	secondary_link	6	trunk_link
2	tertiary	6	bridleway
2	tertiary_link	7	unknown
3	motorway	7	unclassified
3	motorway_link	8	footway
4	living_street	8	path
4	residential	8	pedestrian
4	steps		
4	service		
4	cycleway		

Table S6. Point of Interest classification.

Class	Description	Class	Description
01	automobile service	03	health care service
01	car sale	03	accommodation service
01	vehicle maintenance and repair	03	serviced apartment
01	Motorcycle service	04	tourist attraction
01	transportation facilities service	05	education and culture service
02	catering service	06	government organization
02	shopping service	06	financial and insurance service
03	life services	06	incorporated business
03	spot and leisure services	07	factory

Table S7. The α of bivariate test between each parameter and PM_{2.5}.

α	Himawari-8 AOD	MOD04	MYD04	Tempc	Pressure	RH	HPBL	U	V	DEM	POI	GDP	TPOP
PM _{2.5}	0	0	0	0	0	0	0	0	0	0	0.03	0.036	0.013

Table S8. The spatial ranges of study regions.

	top_latitude	bottom_latitude	left_longitude	right_longitude
North China	45°N	35°N	110°E	120°E
East China	36°N	26°N	112°E	122°E
South China	30°N	20°N	108°E	118°E
Sichuan Basin	36°N	26°N	100°E	110°E
Shaanxi Province	40°N	30°N	105°E	115°E

Table S9. Major features of previous related studies.

Study	Model	Resolution	Study Area	Sample Validation			Space Validation			Time Validation		
				R ²	RMSE	Slop	R ²	RMSE	Slop	R ²	RMSE	Slop
(Ma et	Two-Stage	0.1° daily	China (2004–2013)	0.79	27.42	0.79	-	-	-	-	-	-

al.												
2016)												
(Fang												
et al.	TSAM	10km daily	China	0.80	22.75	0.79	-	-	-	-	-	-
2016)			(2013.6~2014.5)									
(Wang												
et al.	Linear	0.03° night	Atlanta city	-	-	-	0.45	4.11	1.00	-	-	-
2016)	Regression		(2012.8~2012.10)									
(Wei et												
al.	GWR	3km daily	China(2014)	0.79	18.60	0.83	-	-	-	-	-	-
2016)												
(Li et												
al.	Geoi-DBN	10km daily	China (2015)	0.88	13.03	0.88	0.82	16.42	0.86	-	-	-
2017)												
(Yu et												
al.	Gauss	10km daily	China (2013)	0.81	21.87	0.73	-	-	-	-	-	-
2017)												
(Xiao												
et al.	Multiple	1km daily	Yangtze River Delta	0.81	25.00	0.99	-	-	-	-	-	-
2017)	Imputation	(full coverage)	(2013~2014)									
(He and												
Huang	GTWR	3km daily	China (2015)	0.80	18.00	0.81	0.75	20.73	0.79	0.58	28.24	0.61
2018)												
(Fu et												
al.	Mixed-Effect	0.01° night	Beijing	-	-	-	0.86	32.4	-	-	-	-
2018)			(2013.12~2014.11)									
(Shtein												
et al.	GAM	1km daily	Italy (2013~2015)	-	-	-	0.80	6.06	0.99	-	-	-
2019)												
(Chen												
et al.	SMLM	0.05° hourly	covers most of China	0.85	17.30	0.86	-	-	-	-	-	-
2019)		(daytime)	(2016)									
(Zhang												
et al.	ST-LME	5km hourly	east-central	0.80	-	-	-	-	-	-	-	-
2019)		(daytime)	China(2015.7~2017.7)									
(Wei et												
al.	ST-RF	1km daily	China (2015)	0.85	15.57	0.82	0.83	16.63	0.81	0.63	24.83	0.62
2019)												
(Bi et												
al.	RF	1km daily	New York State	0.82	2.16	1.05	-	-	-	-	-	-
2019)		(full coverage)	(2015)									
(Zhang												
et al.	XGBoost	3km daily	China	0.87	16.33	-	0.86	17.89	-	0.67	25.87	-
2019)		(nearly full coverage)	(2014~2015)									

(Tand et al. 2019)	Two-Stage RF	1km hourly (full day) (full coverage)	Yangtze River Delta (2017)	-	-	-	0.86	12.4	0.81	-	-	-
(Liu et al. 2019)	RF	5km hourly(daytime)	China(2016)	0.86	17.20	0.81	-	-	-	-	-	-
(Jiang et al. 2020)	Two-Stage RF	1km hourly(full day) (full coverage)	China(2018)	0.85	11.02	-	0.74	14.65	-	-	-	-
(Wei et al. 2020)	Enhanced ST-ET	1km daily	China (2017–2018)	0.89	10.33	0.86	0.88	10.93	0.85	-	-	-
(Park et al. 2020)	CNN-RF	12km daily	America (2011)	0.84	2.55	1.04	0.69	3.55	1.00	0.84	2.55	1.05
This study	ST-NN	0.01° hourly (full day)(full coverage)	covers most of China (2017–2020)	0.88	12.98	0.99	0.85	14.33	1.02	0.86	14.69	1.02

References:

- Ma, Z.; Hu, X.; Sayer, A. M.; Levy, R.; Zhang, Q.; Xue, Y.; Tong, S.; Bi, J.; Huang, L.; Liu, Y., Satellite-based spatiotemporal trends in PM_{2.5} concentrations: China, 2004–2013. *Environmental health perspectives* 2016, 124, (2), 184–192.
- Fang, X.; Zou, B.; Liu, X.; Sternberg, T.; Zhai, L., Satellite-based ground PM_{2.5} estimation using timely structure adaptive modeling. *Remote Sensing of Environment* 2016, 186, 152–163.
- Wang, J.; Aegerter, C.; Xu, X.; Szykman, J. J., Potential application of VIIRS Day/Night Band for monitoring nighttime surface PM_{2.5} air quality from space. *Atmospheric environment* 2016, 124, 55–63.
- You, W.; Zang, Z.; Zhang, L.; Li, Y.; Pan, X.; Wang, W., National-scale estimates of ground-level PM_{2.5} concentration in China using geographically weighted regression based on 3 km resolution MODIS AOD. *Remote Sensing* 2016, 8, (3), 184.
- Li, T.; Shen, H.; Yuan, Q.; Zhang, X.; Zhang, L., Estimating ground-level PM_{2.5} by fusing satellite and station observations: a geo-intelligent deep learning approach. *Geophysical Research Letters* 2017, 44, (23), 11,985–11,993.
- Yu, W.; Liu, Y.; Ma, Z.; Bi, J., Improving satellite-based PM_{2.5} estimates in China using Gaussian processes modeling in a Bayesian hierarchical setting. *Scientific reports* 2017, 7, (1), 1–9.
- Xiao, Q.; Wang, Y.; Chang, H. H.; Meng, X.; Geng, G.; Lyapustin, A.; Liu, Y., Full-coverage high-resolution daily PM_{2.5} estimation using MAIAC AOD in the Yangtze River Delta of China. *Remote Sensing of Environment* 2017, 199, 437–446.
- He, Q.; Huang, B., Satellite-based mapping of daily high-resolution ground PM_{2.5} in China via space-time regression modeling. *Remote Sensing of Environment* 2018, 206, 72–83.
- Fu, D.; Xia, X.; Duan, M.; Zhang, X.; Li, X.; Wang, J.; Liu, J., Mapping nighttime PM_{2.5} from VIIRS DNB using a linear mixed-effect model. *Atmospheric Environment* 2018, 178, 214–222.
- Shtein, A.; Kloog, I.; Schwartz, J.; Silibello, C.; Michelozzi, P.; Gariazzo, C.; Viegi, G.; Forastiere, F.; Karnieli, A.; Just, A. C., Estimating daily PM_{2.5} and PM₁₀ over Italy using an ensemble model. *Environmental science &*

technology 2019, 54, (1), 120-128.

Chen, J.; Yin, J.; Zang, L.; Zhang, T.; Zhao, M., Stacking machine learning model for estimating hourly PM_{2.5} in China based on Himawari 8 aerosol optical depth data. *Science of The Total Environment* 2019, 697, 134021.

Zhang, T.; Zang, L.; Wan, Y.; Wang, W.; Zhang, Y., Ground-level PM_{2.5} estimation over urban agglomerations in China with high spatiotemporal resolution based on Himawari-8. *Science of the total environment* 2019, 676, 535-544.

Wei, J.; Huang, W.; Li, Z.; Xue, W.; Peng, Y.; Sun, L.; Cribb, M., Estimating 1-km-resolution PM_{2.5} concentrations across China using the space-time random forest approach. *Remote Sensing of Environment* 2019, 231, 111221.

Bi, J.; Belle, J. H.; Wang, Y.; Lyapustin, A. I.; Wildani, A.; Liu, Y., Impacts of snow and cloud covers on satellite-derived PM_{2.5} levels. *Remote sensing of environment* 2019, 221, 665-674.

Chen, Z.-Y.; Zhang, T.-H.; Zhang, R.; Zhu, Z.-M.; Yang, J.; Chen, P.-Y.; Ou, C.-Q.; Guo, Y., Extreme gradient boosting model to estimate PM_{2.5} concentrations with missing-filled satellite data in China. *Atmospheric Environment* 2019, 202, 180-189.

Tang, D.; Liu, D.; Tang, Y.; Seyler, B. C.; Deng, X.; Zhan, Y., Comparison of GOCI and Himawari-8 aerosol optical depth for deriving full-coverage hourly PM_{2.5} across the Yangtze River Delta. *Atmospheric Environment* 2019, 217, 116973.

Liu, J.; Weng, F.; Li, Z., Satellite-based PM_{2.5} estimation directly from reflectance at the top of the atmosphere using a machine learning algorithm. *Atmospheric Environment* 2019, 208, 113-122.

Jiang, T.; Chen, B.; Nie, Z.; Ren, Z.; Xu, B.; Tang, S., Estimation of hourly full-coverage PM_{2.5} concentrations at 1-km resolution in China using a two-stage random forest model. *Atmospheric Research* 2021, 248, 105146.

Wei, J.; Li, Z.; Cribb, M.; Huang, W.; Xue, W.; Sun, L.; Guo, J.; Peng, Y.; Li, J.; Lyapustin, A., Improved 1 km resolution PM_{2.5} estimates across China using enhanced space-time extremely randomized trees. *Atmospheric Chemistry and Physics* 2020, 20, (6), 3273-3289.

Park, Y.; Kwon, B.; Heo, J.; Hu, X.; Liu, Y.; Moon, T., Estimating PM_{2.5} concentration of the conterminous United States via interpretable convolutional neural networks. *Environmental Pollution* 2020, 256, 113395.

Table S10. The influences of different data quality treatments on the performance of the model.

train	test	RMSE	MAE	Slope	R-square
without empty data	without empty data	16.53	10.10	0.98	0.87
	without outlier data	14.62	9.55	0.96	0.87
without outlier data	without empty data	18.24	10.46	1.06	0.84
	without outlier data	14.30	9.46	1.00	0.87

Table S11. Data quality control status.

	2017(N)		2018(N)		2019(N)		2020(N)		Rate
	outlier	not null	outlier	not null	outlier	not null	outlier	not null	
North China	188547	1340252	186265	1241169	180120	1257882	175359	1228487	0.14
East China	420792	2663647	364102	2525520	395344	2478030	381681	2503516	0.15

South China	325190	1957469	280304	1875939	298656	1865894	342722	1908516	0.16
Sichuan Basin	170788	1132051	168210	1043238	167905	1044349	170819	1062847	0.16
Shaanxi Province	189610	1369405	184997	1280065	184698	1277902	199430	1301866	0.15

Table S12. Statistics of number of stations used for training and testing

	All	Training	Testing	All Sample Number(N)			
	Number(N)	Number(N)	Number(N)	2017	2018	2019	2020
North China	176	150	26	1340252	1241169	1257882	1228487
East China	343	308	35	2663647	2525520	2478030	2503516
South China	237	213	24	1957469	1875939	1865894	1908516
Sichuan Basin	145	130	15	1132051	1043238	1044349	1062847
Shaanxi Province	177	159	18	1369405	1280065	1277902	1301866

Table.S13. Validation results for different scales of spatial region mask.

Train Area	36°~44°N		27°~35°N													
	111°~119°E		123°~121°E													
Mask Area	38.2°~40.2°N		29°~33°N		30°~33°N		31°~33°N		32°~33°N		32°~33°N		31°~32°N		31°~32°N	
	114.1°~116.1°E		116°~120°E		117°~120°E		118°~120°E		118°~119°E		119°~120°E		118°~119°E		119°~120°E	
R-square	Num ber	Rate (%)	Nu mbe r	Rate (%)	Num ber	Rate (%)	Num ber	Rate (%)	Num ber	Rate (%)	Num ber	Rate (%)	Num ber	Rate (%)	Num ber	Rate (%)
<0.5	/	/	5	0.05	1	0.01	/	/	/	/	/	/	/	/	/	/
0.5~0.6	/	/	9	0.09	4	0.05	/	/	/	/	/	/	/	/	/	/
0.6~0.65	/	/	14	0.14	6	0.08	/	/	/	/	/	/	/	/	/	/
0.65~0.7	/	/	34	0.35	21	0.28	2	0.05	/	/	/	/	/	/	/	/
0.7~0.75	1	0.17	24	0.24	24	0.32	9	0.22	/	/	1	0.12	/	/	2	0.18
0.75~0.8	5	0.83	6	0.06	10	0.13	19	0.48	3	0.25	6	0.76	/	/	5	0.45
>0.8	/	/	6	0.06	10	0.13	10	0.25	9	0.75	1	0.12	9	1	4	0.37

Table.S14. Hourly validation of Near Real Time model (trained with data from 2017 to 2020 and test with 2020).

R-squre	Number	CNEMC mean	ST-NN mean
<0.4	10	16.26	19.81

0.4~0.45	8	35.28	30.51
0.45~0.5	21	35.73	35.44
0.5~0.55	26	41.17	43.72
0.55~0.6	30	40.70	43.96
0.6~0.65	20	39.47	41.74
0.65~0.7	26	41.26	45.04
>0.7	9	42.30	47.40

Table.S15. Assess the ability of the model to capture different levels of contamination through accuracy and precision.

	North China NRT model ($>75\mu\text{g}/\text{m}^3$)		29°~33°N,116°~120°E mask ($>75\mu\text{g}/\text{m}^3$)		30°~33°N,117°~120°E mask ($>75\mu\text{g}/\text{m}^3$)		31°~33°N,118°~120°E mask ($>75\mu\text{g}/\text{m}^3$)	
value	Number		Number		Number		Number	
	accuracy	precision	accuracy	precision	accuracy	precision	accuracy	precision
<0.4	/	14	/	9	/	0	/	1
0.4~0.5	/	6	/	16	/	1	/	0
0.5~0.6	/	15	/	21	/	6	/	4
0.6~0.7	/	28	/	28	/	13	/	13
0.7~0.8	/	28	/	14	/	24	/	11
0.8~0.9	31	22	3	7	/	20	/	8
>0.9	100	18	95	3	82	18	45	8

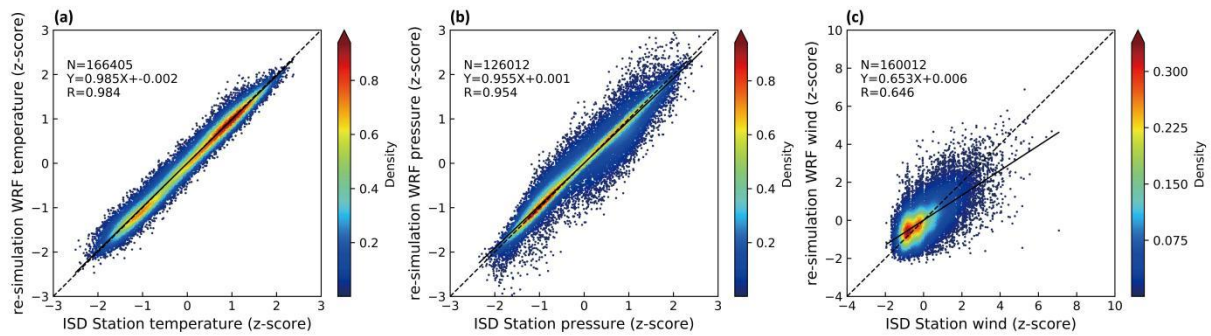


Figure. S1. Validation of meteorological parameters simulated by WRF with observation data at ISD (Integrated Surface Database) stations. (a) temperature. (b) pressure. (c) wind speeds.

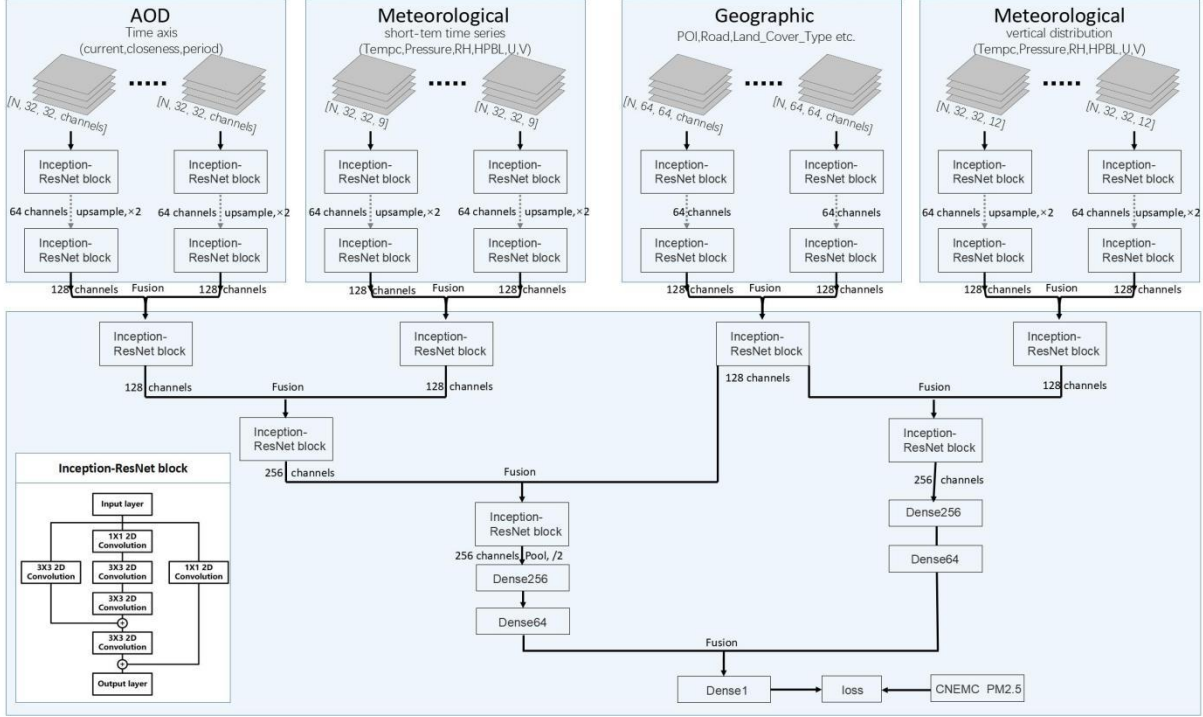


Figure. S2. The architecture of the ST-NN model. Inputs data include AOD, meteorological

data and geographic data. All the input variables have the 4-D dimensions as $[N, \text{lat_size},$

$\text{lon_size}, \text{channel}]$. N means the batch size, lat_size and lon_size means the scale of the data at

latitude and longitude, channels represent the types or the height/time dimension of the data.

Considering the computational efficiency and the generalization ability of the model, we

choose N as 4. First, feature extraction was used for individual data by Inception-ResNet,

which is an efficient feature extraction process. After it, we up-sampled the data at $0.05^\circ \times$

0.05° resolution using the transposed convolution layer, which is a learning-based

up-sampling method. We used the strides as 2 and a 2×2 convolution kernel to double size of

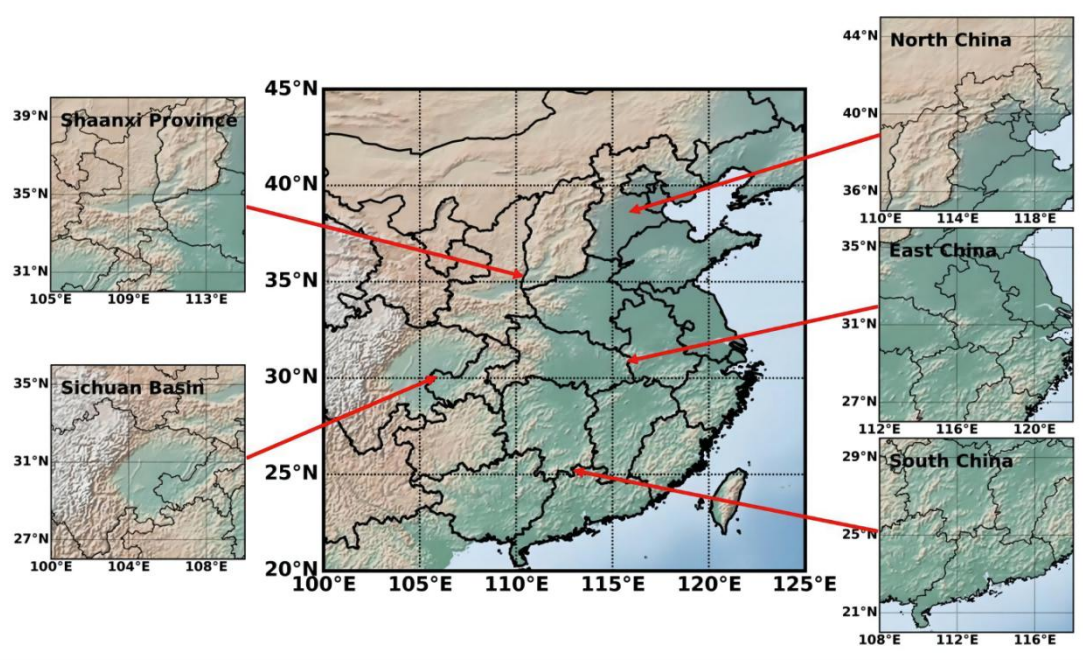
the input data. Accordingly, all data had the same size. Then we mined the characteristics of

each variable and fused the data with same types by concatenate layer. Then the temporal and

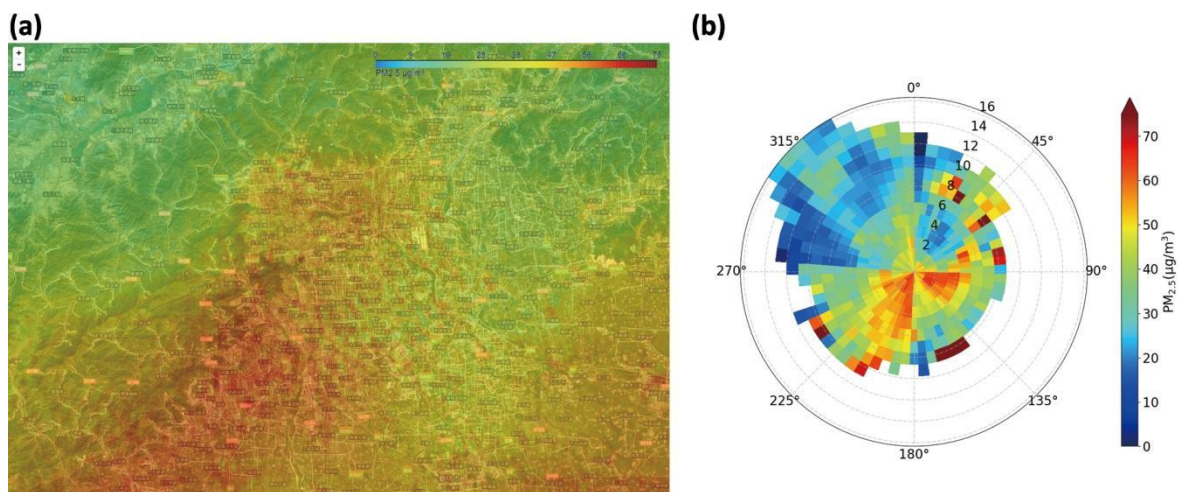
spatial features were extracted by fusing the time-series of aerosol and meteorological data

with the geographic information data. The final result was obtained through the fully

213 connected layer.



214
215 **Figure. S3.** Locations and spatial range of major study regions. Study regions include North
216 China, East China, South China, Sichuan Basin and Shaanxi Province.



218
219 **Figure. S4.** The annual average distribution of $PM_{2.5}$ in Beijing (a). b is a rose, with radius
220 representing wind speed and the color indicating mean $PM_{2.5}$ concentrations. 0° is due north
221 and 90° is due east. It can be seen that the main pollution comes from the southwest,
222 significantly influenced by topography and transmission.

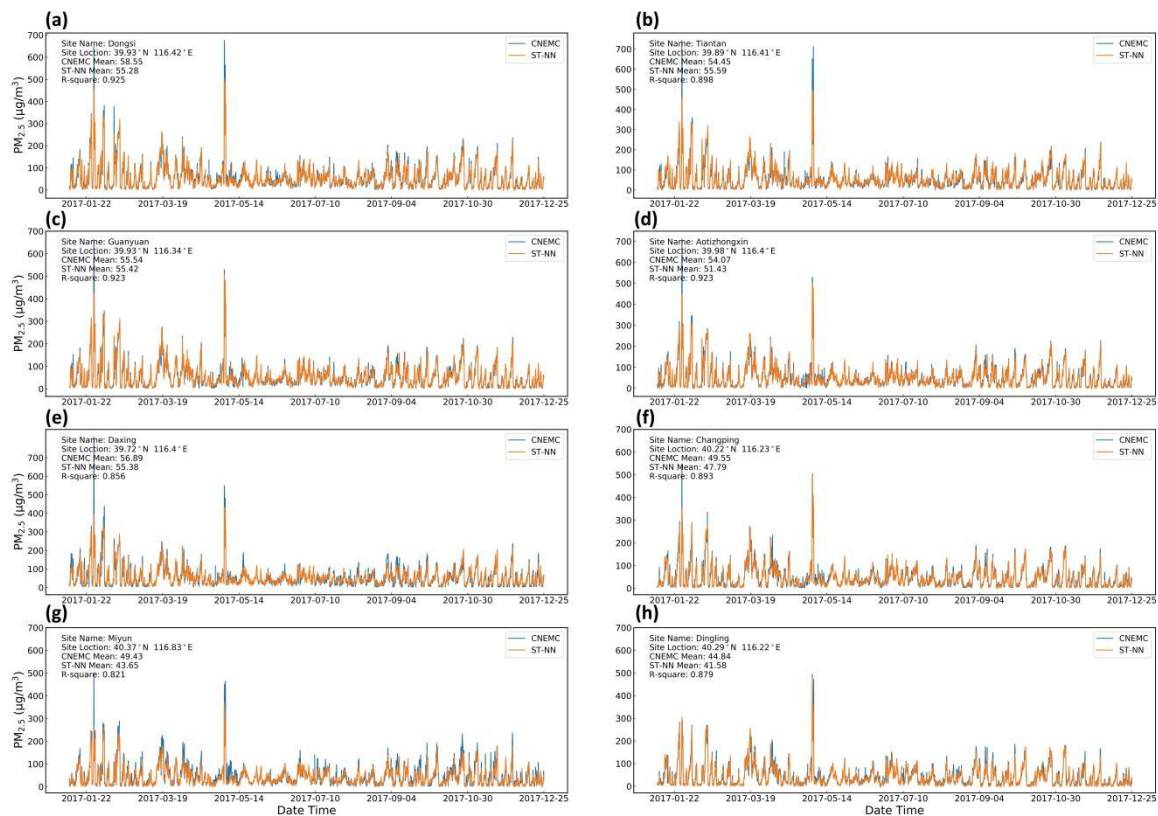


Figure. S5. ST-NN model predicted and ground-level observed (not used in training) time

series of PM_{2.5} in Beijing stations. (a) Dongsì station in Beijing. (a) Tiantan station in Beijing.

(c) Guanyuan station in Beijing. (d) Aotizhognxin station in Beijing. (e) Daxing station in

Beijing. (f) Changping station in Beijing. (g) Miyun station in Beijing. (h) Dingling station in

Beijing. (a-d) stations are in city, and (e-h) are rural stations.

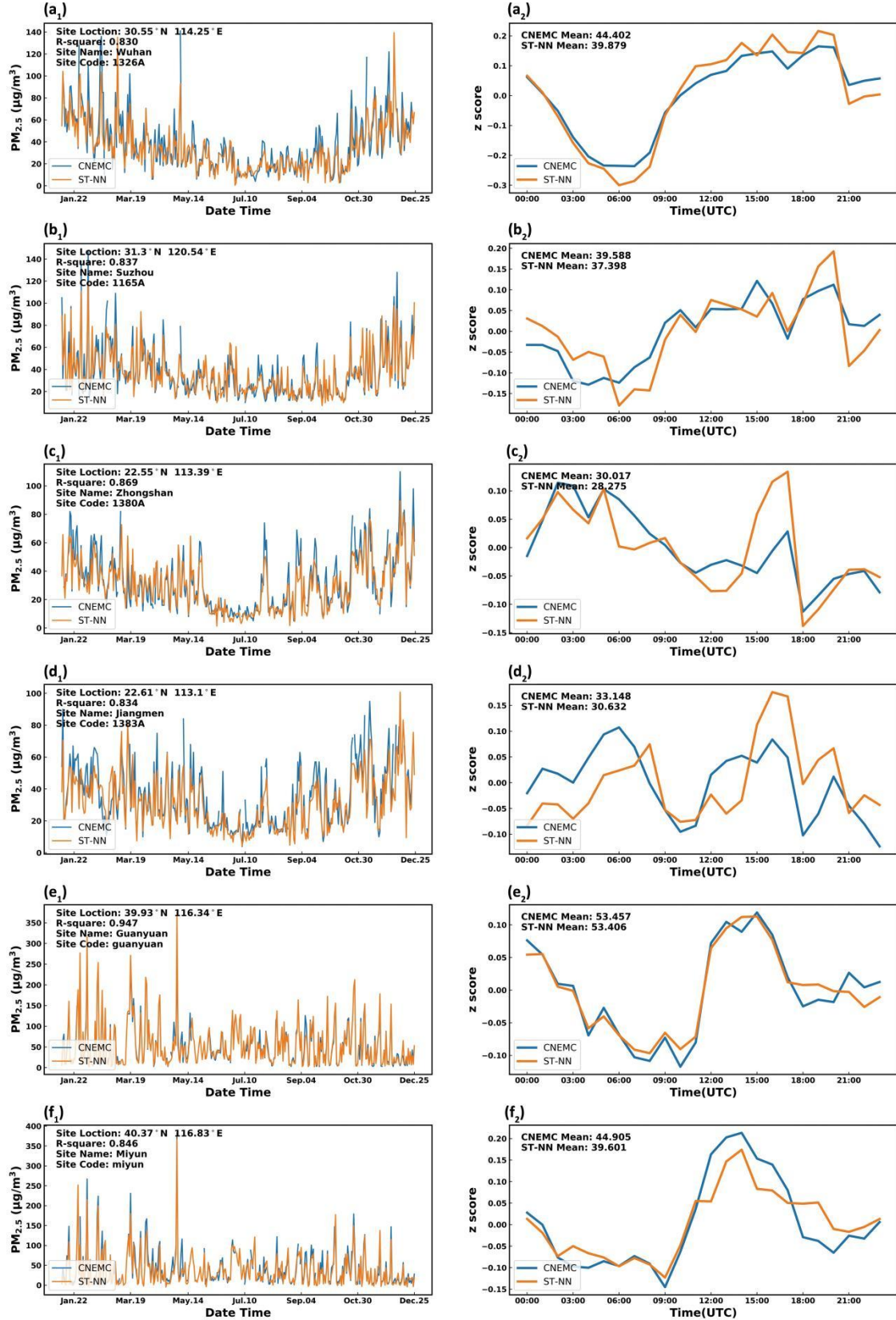


Figure. S6. ST-NN model predicted and ground-level observed (not used in training) time series (2017) of PM_{2.5} in China, and comparisons of their diurnal features. Left column: ST-NN model predicted and observed time series of PM_{2.5} in Wuhan (a₁), Suzhou (b₁),

Zhongshan (c_1), Jiangmen (d_1), Guanyuan in Beijing (e_1), Miyun in Beijing (f_1); Right column:
 ST-NN model predicted and observed diurnal variation of $PM_{2.5}$ in Wuhan (a_2), Suzhou (b_2),
 Zhongshan (c_2), Jiangmen (d_2), Guanyuan in Beijing (e_2), Miyun in Beijing (f_2). Its vertical
 axis is the z-score coordinate. $z - \text{score} = \frac{x - \mu}{\sigma}$, μ is the sample mean and σ is the sample
 standard deviation.

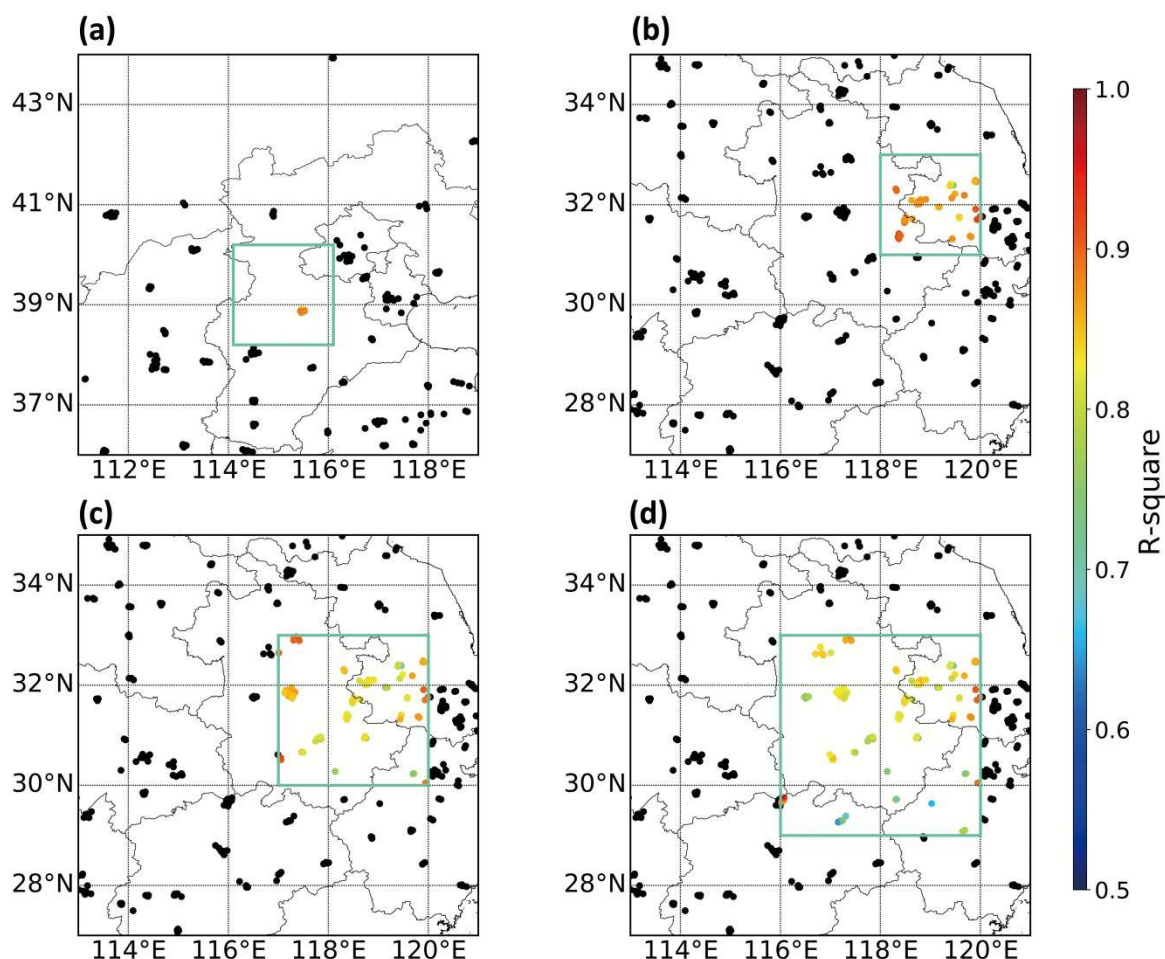


Figure. S7. The block distribution of the regional mask validation. Validation was carried
 out for different spatial mask scales, the black points are the training sites, and the
 R-square distribution of the validation sites is enclosed by the solid blue line.

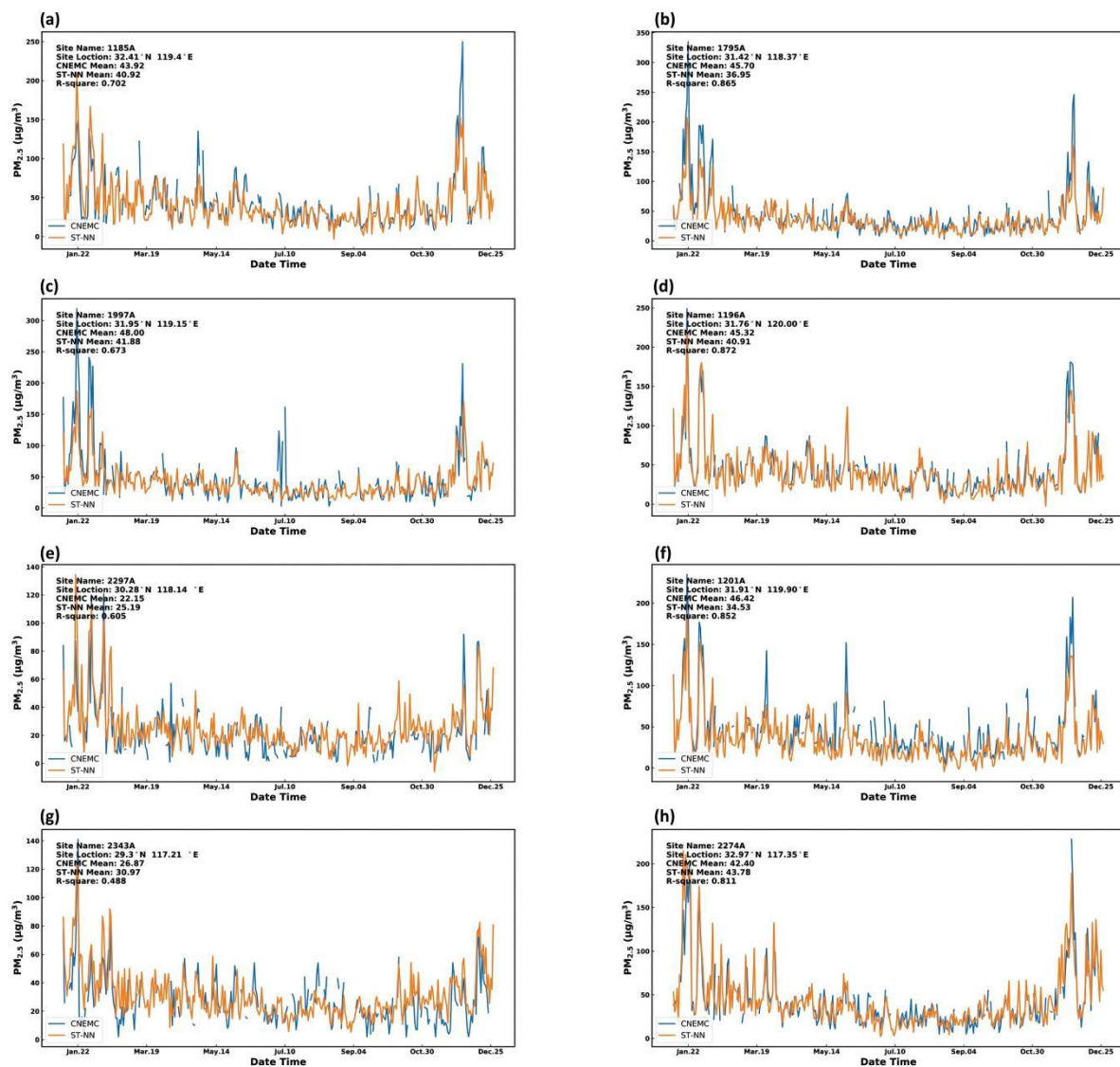


Figure. S8. Time series of the regional mask performed (Figure.S6b,c,d). (a,b) are the 1°x1° mask validation in the East China. (c,d) are the results of 2°x2° mask validation in the East China. (e,f) are the validation of 3°x3° mask in East China. (g,h) are the validation of 4°x4° mask in East China. And (a,b,c,g) are urban stations. (d,e,f,h) are rural stations.

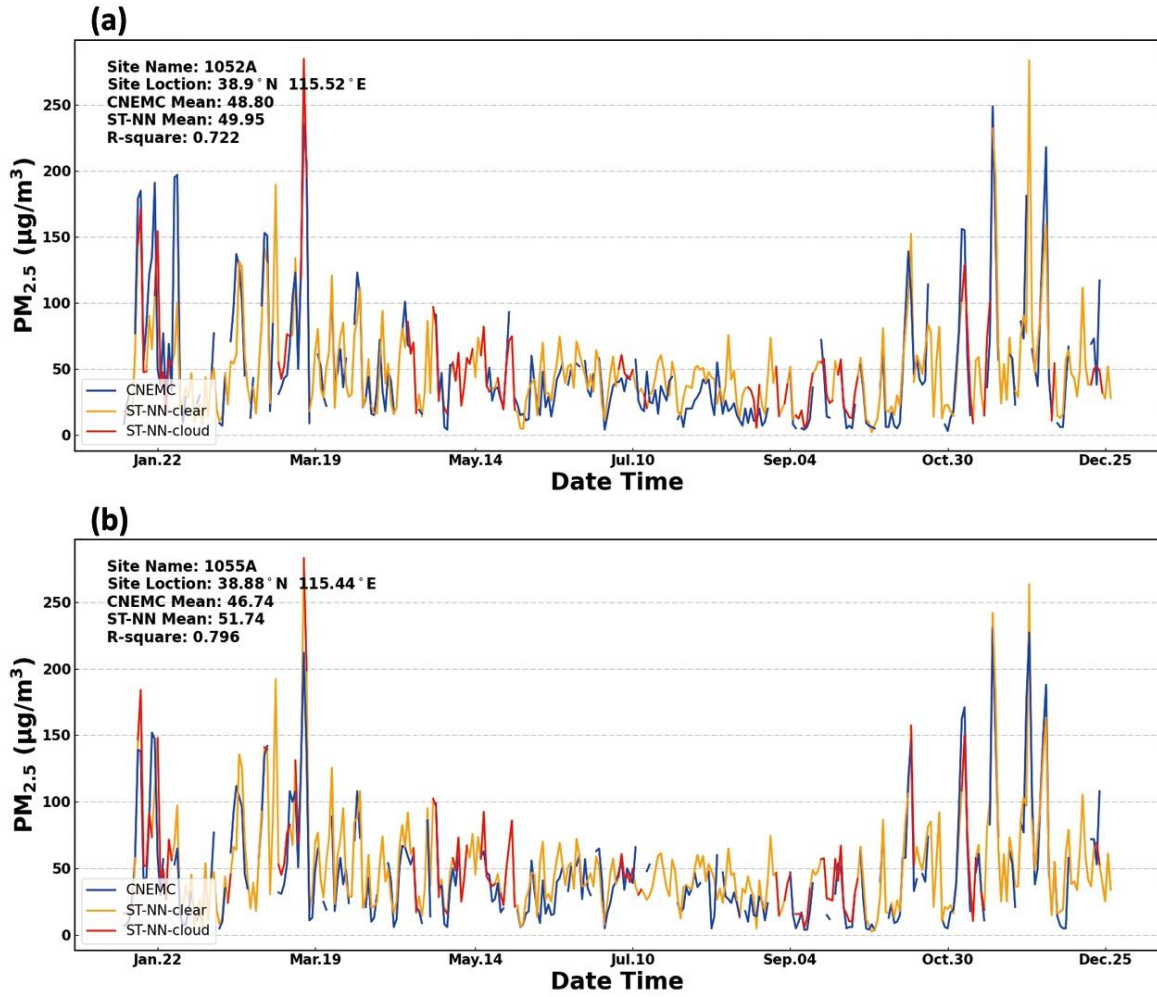


Figure. S9. Time series of the regional mask performed (Figure.S6a), they are the $2^\circ \times 2^\circ$ mask validation in the North China. The blue line is the CNEMC data, the orange line is the ST-NN result for clear day, the red line is the ST-NN result for cloudy day. a is a rural station, b is an urban station.

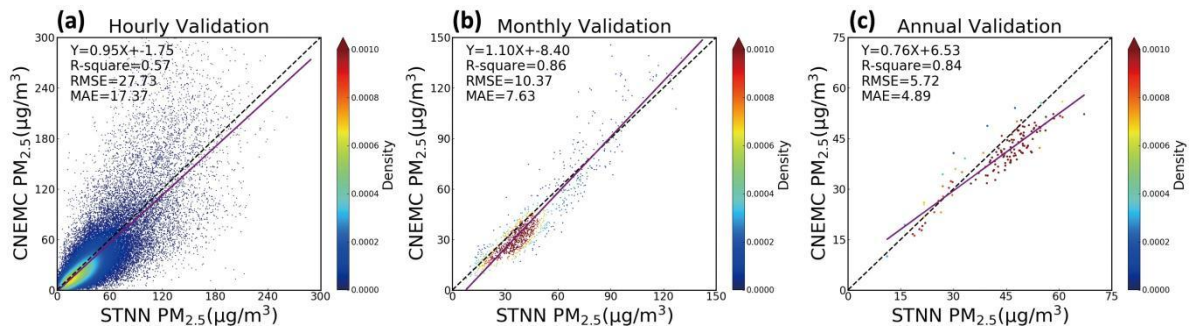


Figure. S10. Density scatterplots of the ST-NN model (trained with data from 2017 to

2020 and test with 2020) with hourly(a),monthly(b),annual(c) validation. The fitting line is in purple, and the 1:1 standard line is the black dotted line.

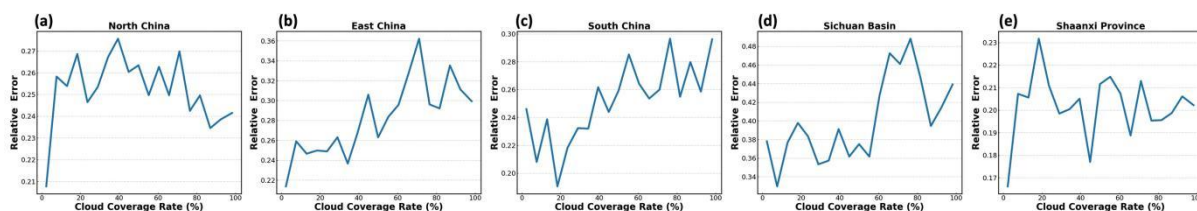


Figure. S11. Relative error of cross validation under different cloud coverage rates.

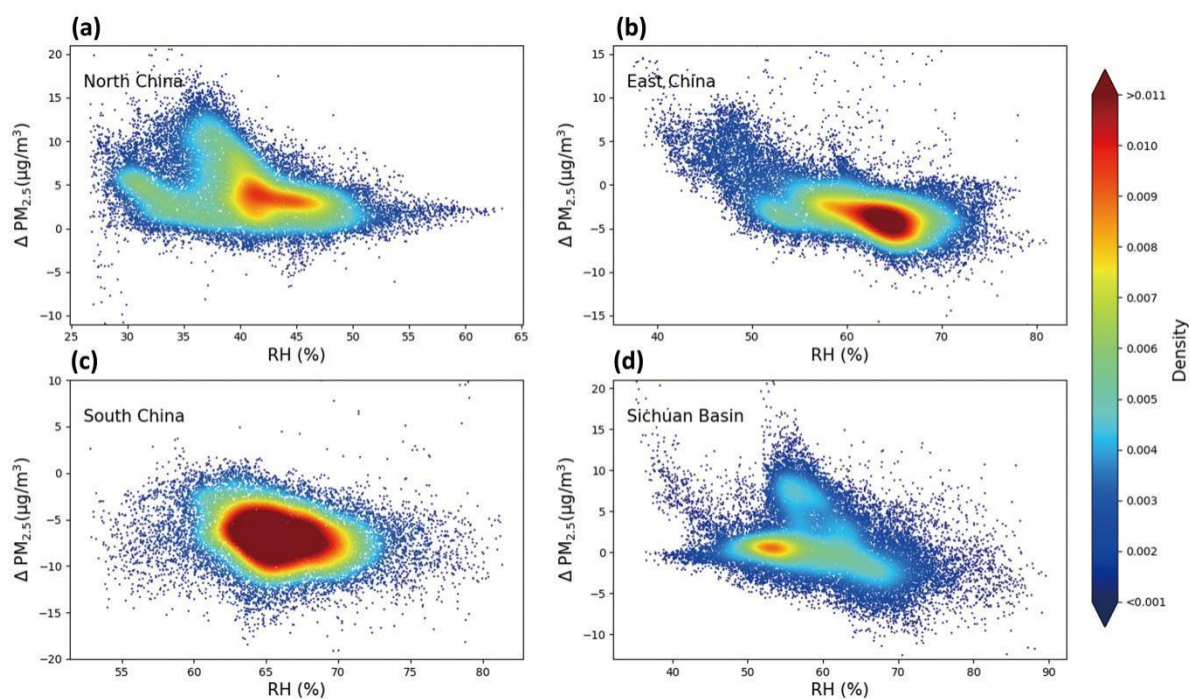


Figure. S12. The density distribution diagram of changes in predicted $PM_{2.5}$ concentrations as a function of relative humidity in marked cloudy conditions. (a) North China. (b) East China. (c) South China. (d) Sichuan Basin.

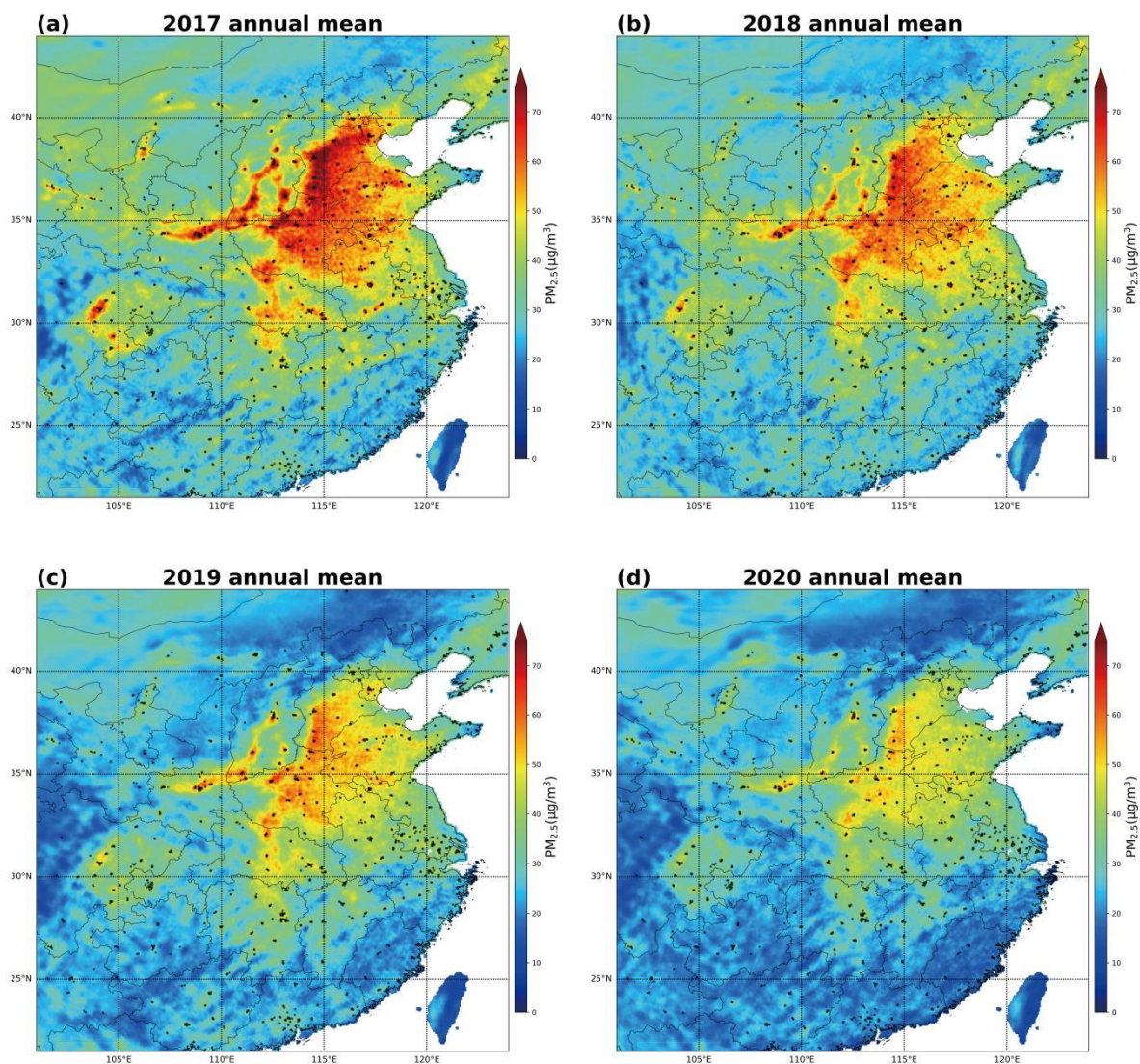


Figure. S13. The distribution of predicted annual mean concentrations of PM_{2.5} and the locations of monitoring sites.

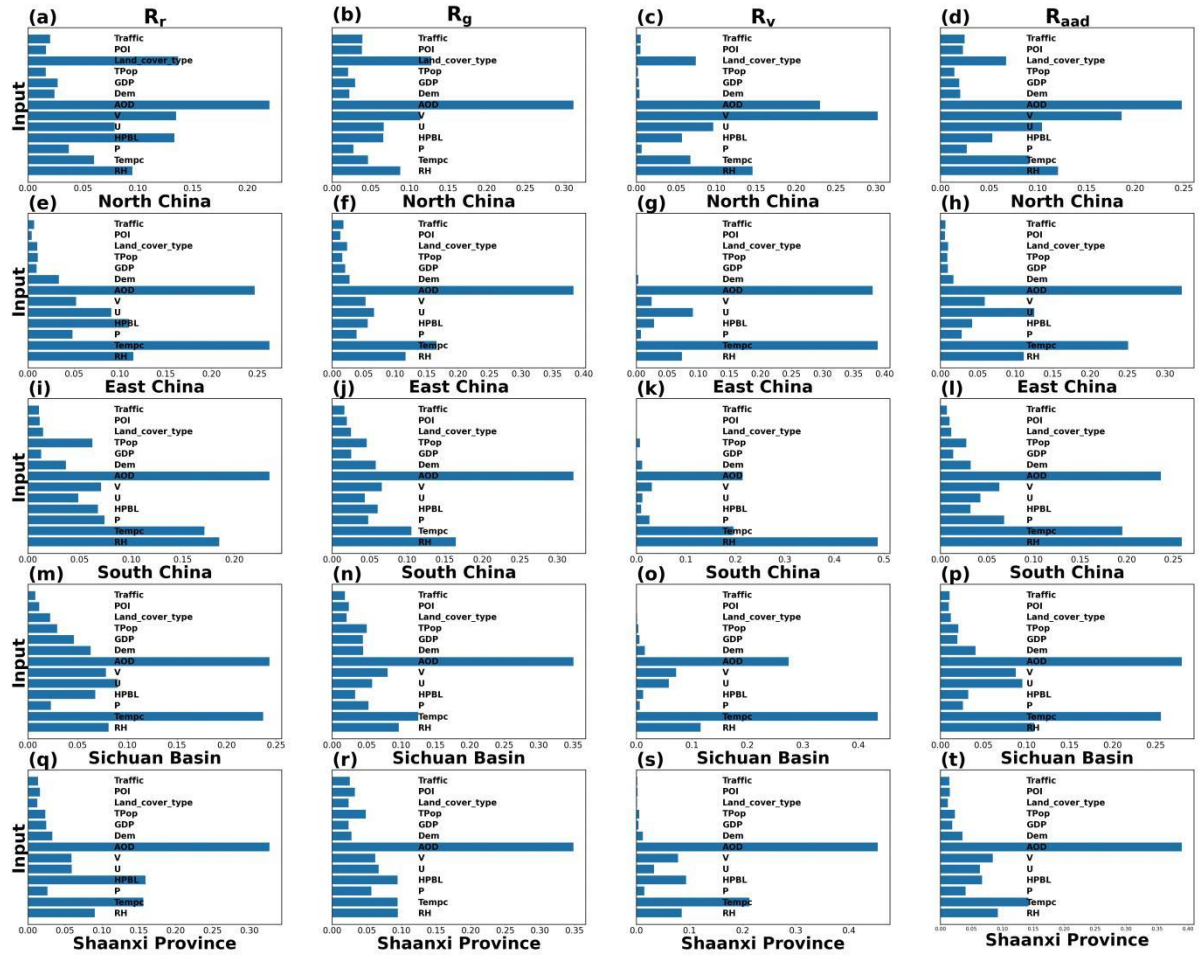


Figure. S14. Relative importance indicators (R_r : Relative range; R_g : Relative gradient; R_v : Relative variance; R_{AAD} : Relative average absolute deviation) of input variables for different regions. (a-d) North China. (e-h) East China. (i-l) South China. (m-p) Sichuan Basin. (q-t) Shaanxi Province.

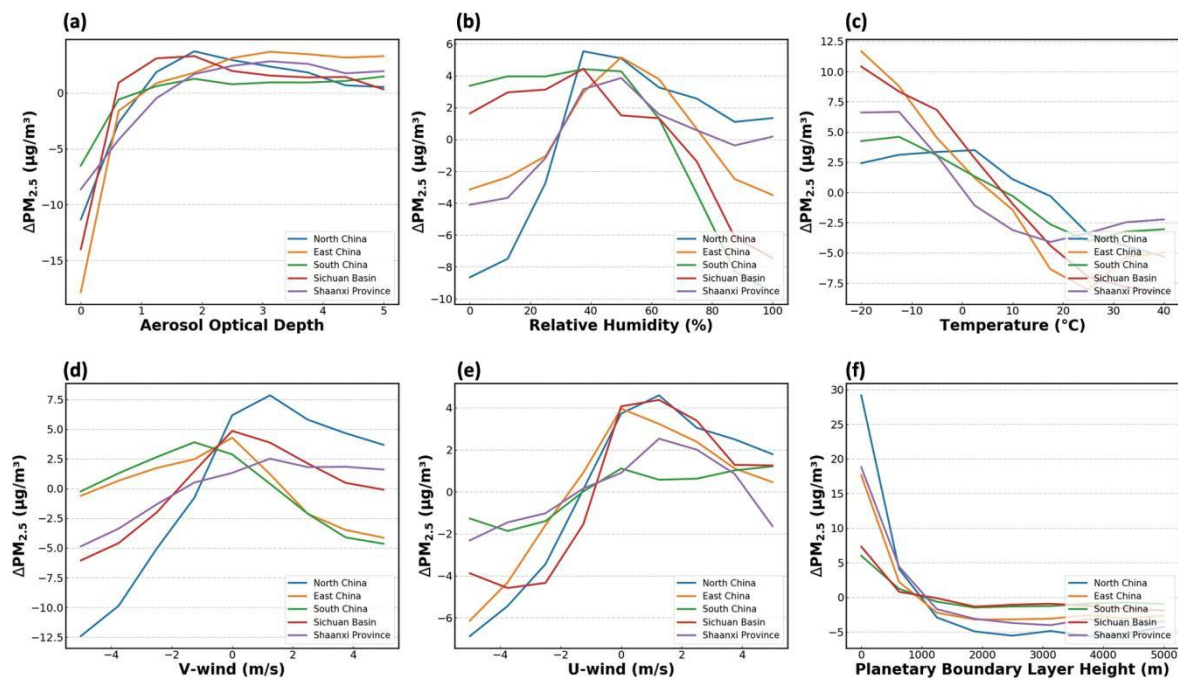


Figure. S15. Results of sensitivity analysis of key variables. The influence of relative humidity is mainly due to the hygroscopic growth of $PM_{2.5}$ and the wet removal which is more pronounced in North China. The effect of temperature is mainly seasonal. Low boundary layer pressure leads to higher surface $PM_{2.5}$ concentrations.

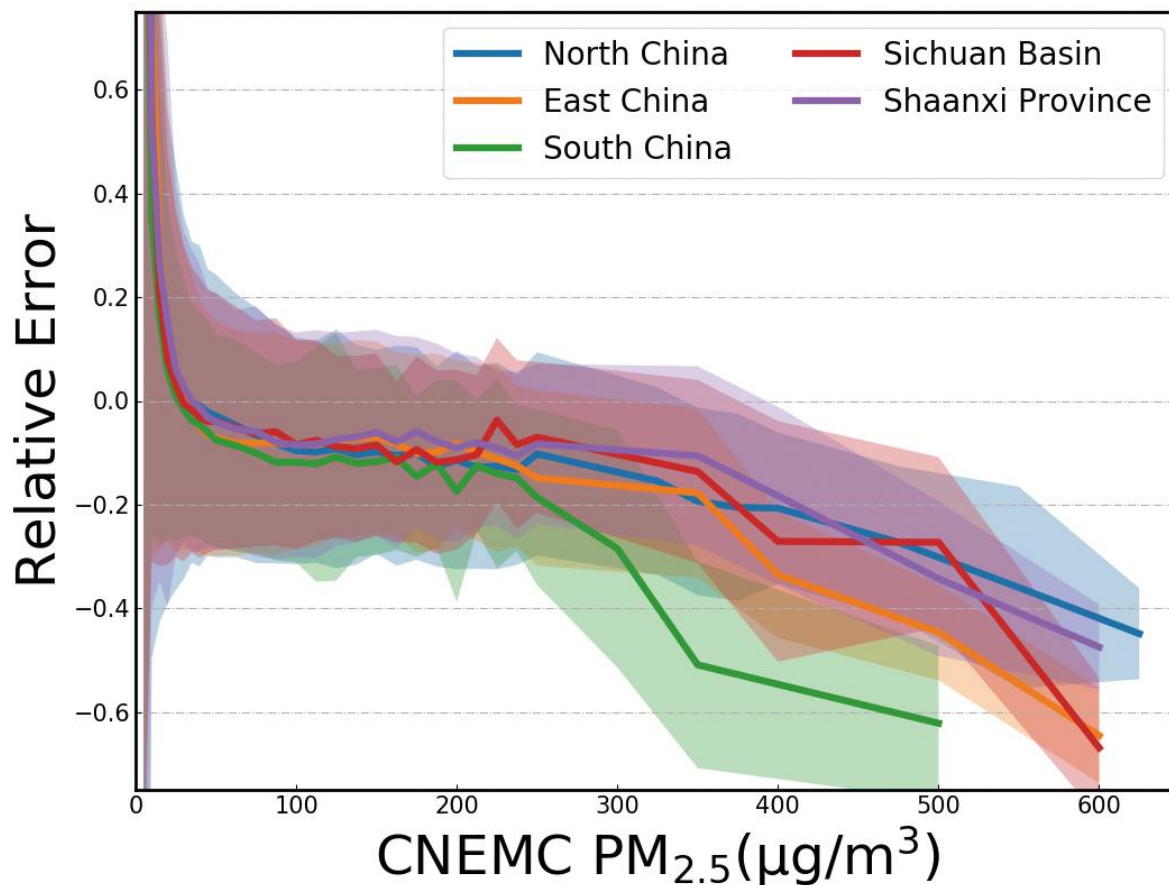


Figure. S16. Relative error varies with PM_{2.5} concentrations in different regions. Five lines with different colors represent errors for North China, East China, South China, Sichuan Basin, and Shaanxi Province.

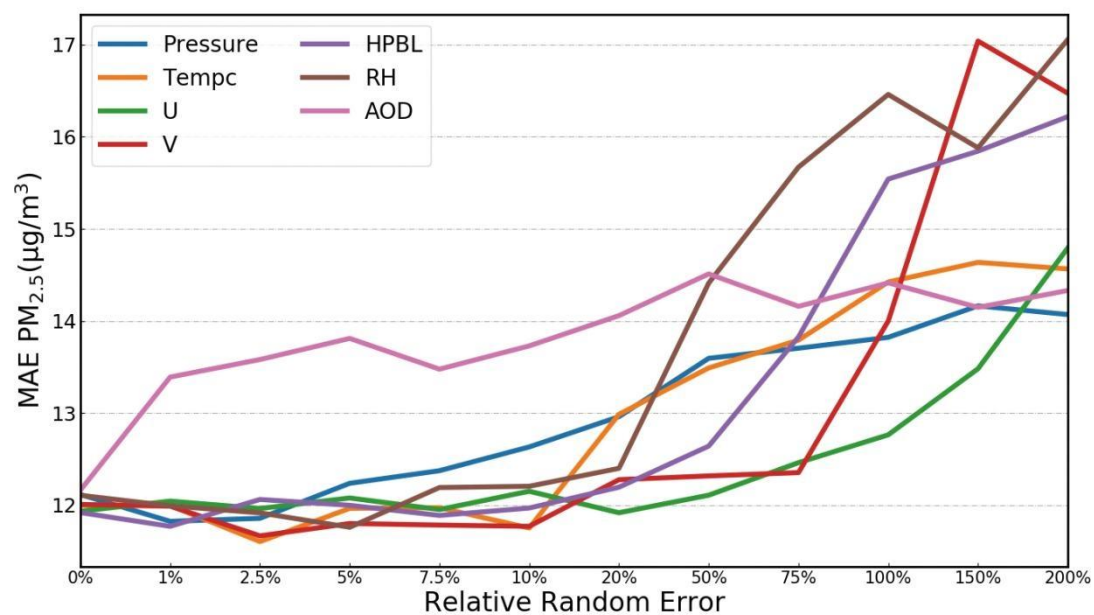


Figure. S17. The relationship between the mean absolute error of the model and the relative error of different input data. Seven lines with different colors represent model inputs: pressure, temperature, zonal wind (U), meridional wind (V), boundary layer height, relative humidity, and AOD.

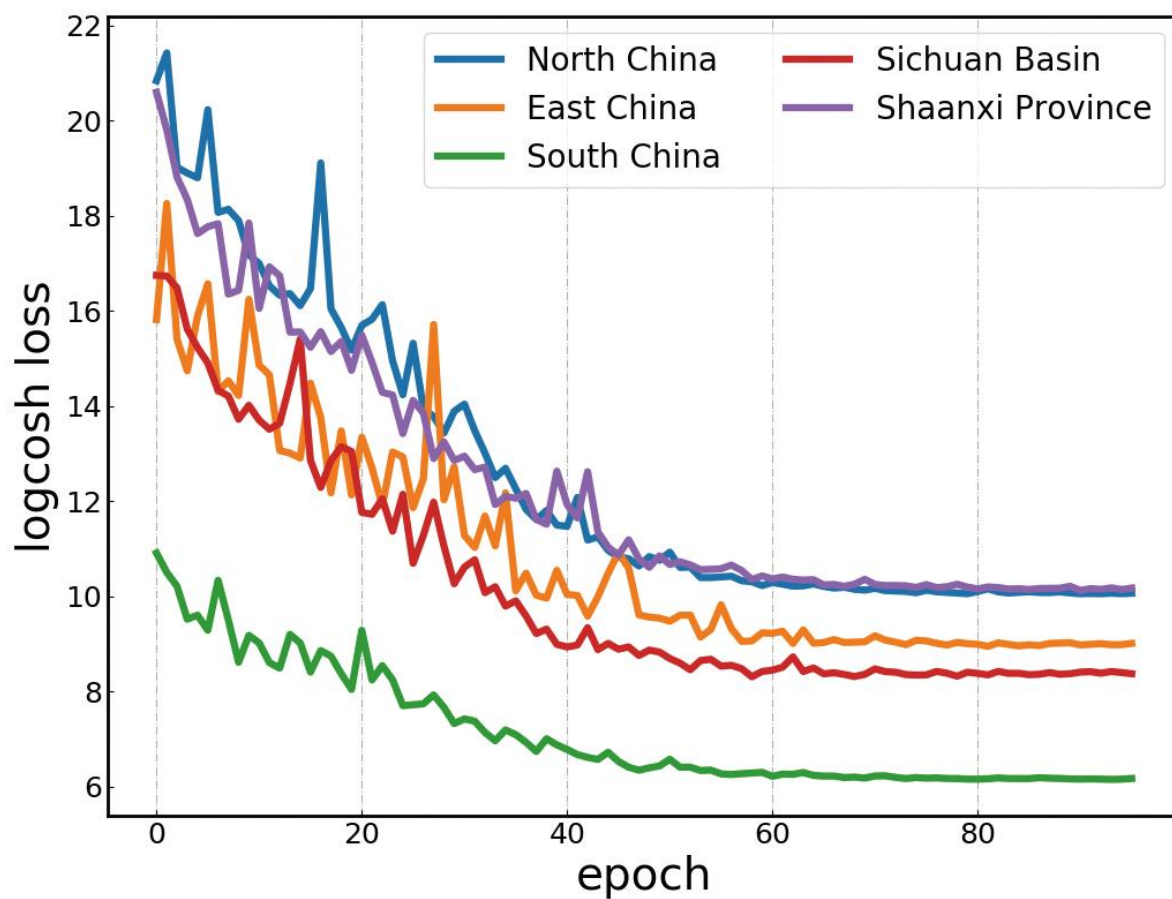


Figure. S18. The performance of the validation data logcosh loss function for models built for different regions. Five lines with different colors represent results for North China, East China, South China, Sichuan Basin, and Shaanxi Province.

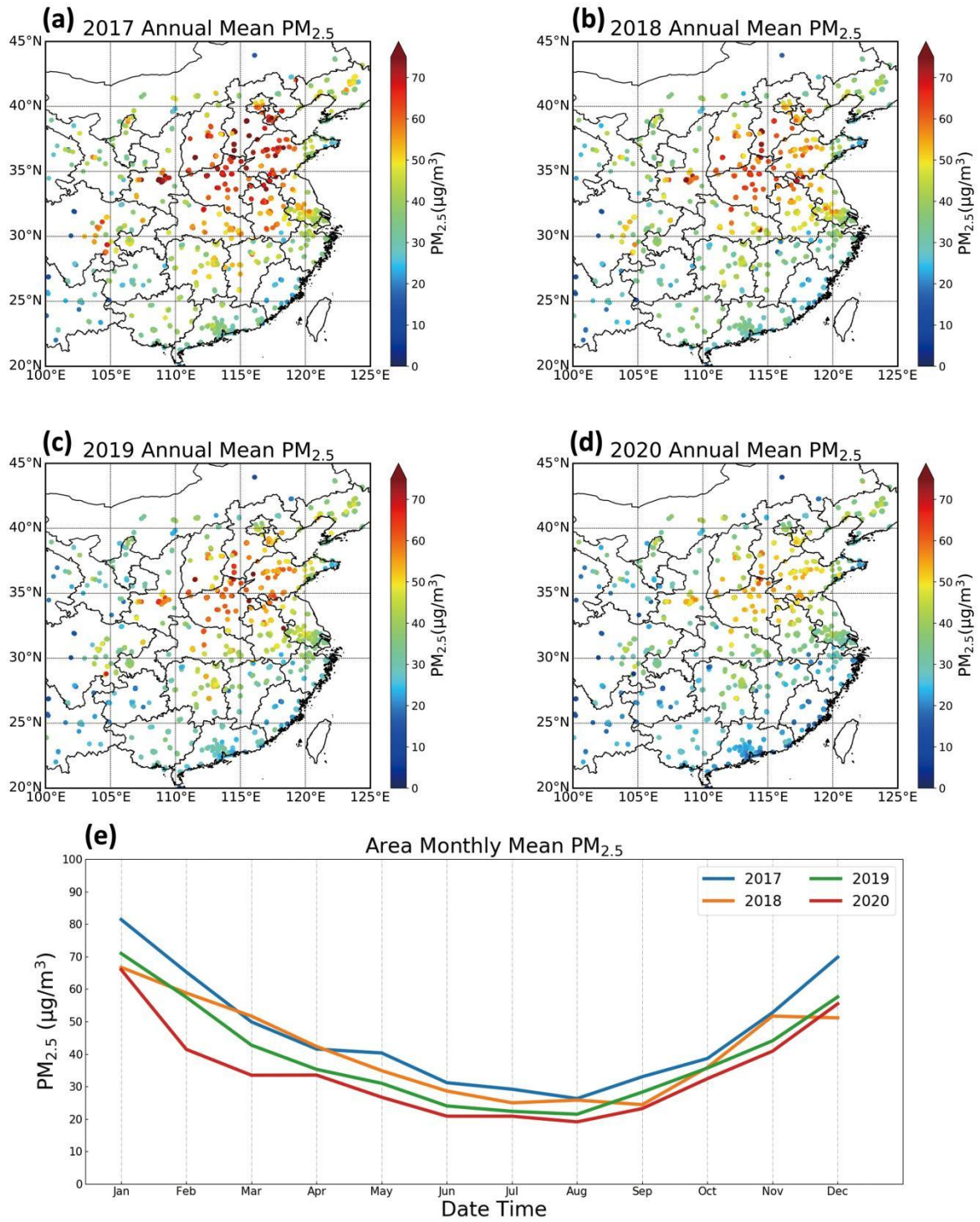


Figure. S19. The spatiotemporal distribution of CNEMC observed $PM_{2.5}$ concentrations. (a) Year 2017. (b) Year 2018. (c) Year 2019. (d) Year 2020. (e) Monthly variations.